Ann. Phys. (Berlin) **523**, No. 1 – 2, 157 – 167 (2011) / **DOI** 10.1002/andp.201000096

Lattice dynamics of $ZnAl_2O_4$ and $ZnGa_2O_4$ under high pressure

S. López-Moreno[1,*], **P. Rodríguez-Hernández**[1], **A. Muñoz**[1], **A. H. Romero**[2], **F. J. Manjón**[3], **D. Errandonea**[4], **E. Rusu**[5], and **V. V. Ursaki**[5]

[1] Departamento de Física Fundamental II, MALTA Consolider Team, Instituto de Materiales y Nanotecnología Universidad de La Laguna, La Laguna 38205, Tenerife, Spain
[2] CINVESTAV-Queretaro Libramiento Norponiente No 2000 Real de Juriquilla 76230 Queretaro, Qro, México
[3] Instituto de Diseño para la Fabricación y Producción Automatizada, MALTA Consolider Team, Universitat Politècnica de València, 46022 Valencia, Spain
[4] Fundación General de la Universidad de Valencia ICMUV, MALTA Consolider Team, Edificio de Investigación, C/Dr. Moliner 50, Burjassot, 46100 Valencia, Spain
[5] Institute of Applied Physics, Academy of Sciences of Moldova, 2028 Chisinau, Moldova

Received 31 July 2010, revised 18 September 2010, accepted 27 September 2010
Published online 2 November 2010

Key words Lattice dynamics, phonon, *ab initio*, spinel structure, high pressure.

This article is dedicated to Manuel Cardona.

In this work we present a first-principles density functional study of the vibrational properties of $ZnAl_2O_4$ and $ZnGa_2O_4$ as function of hydrostatic pressure. Based on our previous structural characterization of these two compounds under pressure, herewith, we report the pressure dependence on both systems of the vibrational modes for the cubic spinel structure, for the $CaFe_2O_4$-type structure (*Pnma*) in $ZnAl_2O_4$ and for marokite (*Pbcm*) $ZnGa_2O_4$. Additionally we report a second order phase transition in $ZnGa_2O_4$ from the marokite towards the $CaTi_2O_4$-type structure (*Cmcm*), for which we also calculate the pressure dependence of the vibrational modes at the Γ point. Our calculations are complemented with Raman scattering measurements up to 12 GPa that show a good overall agreement between our calculated and measured mode frequencies.

1 Introduction

AB_2O_4 compounds are ceramics with many interesting mechanic, electric, magnetic and optical properties. Many of these oxides crystallize in the cubic spinel structure ($Fd\bar{3}m$) exemplified by $MgAl_2O_4$. In particular, $ZnAl_2O_4$ and $ZnGa_2O_4$ have gained recent interest for their applications as phosphors because they combine a wide direct band-gap above 3.5 eV, transparent and electroconductive properties, high thermal stability, low acidity, and hydrophobic behavior to be used in many different new dispositives [1–3].

Little is known about the pressure dependence of the mechanical, electrical, and optical properties of $ZnAl_2O_4$ and $ZnGa_2O_4$ spinels. High pressure X-ray diffraction studies of these two compounds have shown that while $ZnAl_2O_4$ does not undergo any phase transition till 43 GPa [4], $ZnGa_2O_4$ undergoes two phase transitions towards the tetragonal spinel ($I4_1/amd$) and marokite (*Pbcm*) structures around 34 and 55 GPa, respectively [5]. Recently, S. López et al. have performed first principles calculations to study the stability of the spinel structures of $ZnAl_2O_4$ and $ZnGa_2O_4$ under high pressure and phonon frequencies in the Γ point at zero pressure [6, 7]. It has been predicted that $ZnAl_2O_4$ should undergo a pressure-induced

* Corresponding author E-mail: lsinhue@yahoo.com.mx

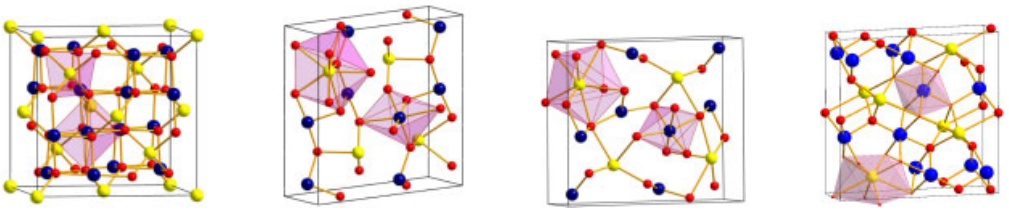

a) b) c) d)

Fig. 1 (online colour at: www.ann-phys.org) Unit cell of the AB_2O_4 structures a) cubic spinel, b) marokite-type, c) $CaFe_2O_4$-type, and d) $CaTi_2O_4$ structure. The atom color palette for *A*(Zn), *B*(Ga or Al), and O are yellow, blue, and red, respectively.

phase transition from the cubic spinel towards the orthorhombic $CaFe_2O_4$-type (*Pnma*) structure around 38.5 GPa while $ZnGa_2O_4$ should undergo a pressure-induced phase transition from the cubic spinel towards the orthorhombic $CaMn_2O_4$-type (marokite) structure around 33.4 GPa. However, the theoretical study has suggested that a possible phase transition from the cubic spinel towards the tetragonal spinel structure can be explained by the presence of non-hydrostatic conditions. This transition had already been observed in $ZnMn_2O_4$ [8] and $NiMn_2O_4$ [9]. Figure 1 shows the unit cells of the cubic spinel, marokite, $CaFe_2O_4$ and $CaTi_2O_4$ phases.

In this paper, we report a lattice dynamics study of $ZnAl_2O_4$ and $ZnGa_2O_4$ spinels as function of hydrostatic pressure. We report the theoretical pressure dependence of the vibrational modes for the cubic spinel structure for both compounds and for the *Pnma* and *Pbcm* phases in $ZnAl_2O_4$ and $ZnGa_2O_4$, respectively. In addition we report a new calculated second order phase transition in $ZnGa_2O_4$ compound from *Pbcm* towards *Cmcm* ($CaTi_2O_4$-type structure) phase for which we also report the pressure dependence of the vibrational modes. Our calculations are complemented with Raman scattering measurements in both spinels up to 12 GPa.

2 Computational details

Total energy calculations were done within the framework of the density functional theory (DFT) and the projector-augmented wave (PAW) [10, 11] method using the Vienna *ab initio* simulation package (VASP) [12–15]. The exchange and correlation energy was described within the local density approximation (LDA) [16]. We use a plane-wave energy cutoff of 500 eV to ensure a high precision in the calculations. Monkhorst-Pack scheme was employed for the Brillouin-zone (BZ) integrations [17] with meshes of $4 \times 4 \times 4$, $3 \times 9 \times 3$, $8 \times 4 \times 4$, and $8 \times 4 \times 4$, which corresponds to a set of 10, 20, 16 and 16 special k-points in the irreducible Brillouin-zone, for structures: cubic spinel ($Fd\bar{3}m$), and the orthorhombic structures with space groups *Pbcm*, *Pnma* and *Cmcm* respectively. In the relaxed equilibrium configuration, the forces are less than 0.9 meV/Å per atom in each of the cartesian directions. The highly converged results on forces are required for the calculations of the dynamical matrix using the direct force constant approach (or supercell method), as implemented in the PHONON program [18]. The construction of the dynamical matrix at the Γ point is particularly simple and involves separate calculations of the forces in which a fixed displacement from the equilibrium configuration of the atoms within the unit cell is considered. Symmetry aids by reducing the number of such independent distortions to a six independent displacements in the cubic spinel phase. Diagonalization of the dynamical matrix provides both the frequencies of the normal modes and their polarization vectors. It allows us to identify the irreducible representation and the character of the phonon modes at the zone center. The phonon dispersion curves were calculated along several high symmetry directions in the BZ. We use a supercell $2\times2\times2$ times the conventional unit cell which consist of four primitive unit cells. The phonon density of states (PDOS) was obtained by integration of the

phonon frequencies with a very high number of k-points. The specific heat of both spinels were obtained from the calculated PDOS within the harmonic approximation.

Table I in [6] provides the calculated and experimental parameters of the spinel structure of both $ZnAl_2O_4$ and $ZnGa_2O_4$ spinels at ambient pressure. An agreement better than 1% is found between theory and experiment for the calculated parameters. Besides, calculated parameters for the tetragonal spinel and $CaMn_2O_4$ and $CaFe_2O_4$ structures are also provided in Table IV of [6].

3 Experimental details

$ZnAl_2O_4$ ($ZnGa_2O_4$) powder was synthesized by a solid state reaction at high temperature by mixing appropriate quantities of ZnO and Al_2O_3 (Ga_2O_3) precursors and firing at 1400 °C (1100 °C) for 24 h [19, 20]. Chemical and structural analysis have shown the stoichiometric composition of $ZnAl_2O_4$ and $ZnGa_2O_4$ and the presence of traces of impurities (α-Al_2O_3 and β-Ga_2O_3, less than 1% by volume, and ZnO, less than 0.2% by volume). Raman scattering measurements were carried out in powder samples at room temperature (RT) in a JobinYvon LabRAM UV HR microspectrometer using an exciting laser line of 532.12 nm with resolution below 3 cm^{-1} and a power below 10 mW on the sample. Raman measurements under high pressures up to 12 GPa were performed with a diamond-anvil cell (DAC) using a 4:1 methanol-ethanol mixture as pressure-transmitting medium [21] and ruby grains for pressure determination [22].

4 Results and discussion

4.1 Cubic spinel $ZnAl_2O_4$ and $ZnGa_2O_4$

Gahnite ($ZnAl_2O_4$) and zinc gallate ($ZnGa_2O_4$) crystallize at ambient pressure in a diamond-type cubic spinel structure with space group $Fd\bar{3}m$ (227) and have two formula units per primitive unit cell, see Fig. 1. The *A* cations are tetrahedrally coordinated and the *B* cations are in BO_6 octahedra. The Zn atoms are located at the Wyckoff positions, 8a ($1/8$,$1/8$,$1/8$) tetrahedral sites, while Al (or Ga) atoms are located on the 16d ($1/2$,$1/2$,$1/2$) octahedral sites and the oxygen atoms at 32e (*u,u,u*). The spinel crystal structure is characterized only by the lattice parameter *a* and the internal parameter *u*.

According to group theory, cubic spinels have the following phonon modes at the Γ point [23]

$$\Gamma = A_{1g}(R) + E_g(R) + T_{1g} + 3T_{2g}(R) + 2A_{2u} + 2E_u + 5T_{1u}(IR) + 2T_{2u}$$

where R and IR corresponds to Raman- and infrared-active modes, respectively, and where one triply degenerated T_{1u} correspond to acoustic modes. Figure 2 shows the calculated phonon dispersion curves along high symmetry directions in both $ZnAl_2O_4$ and $ZnGa_2O_4$ spinels at ambient pressure and the corresponding phonon density of states (PDOS) are show in Fig. 3.

For the PDOS of $ZnAl_2O_4$ the low-frequency motions are mainly due to Zn ions ($<$250 cm^{-1}), while the phonon modes with frequencies over 250 cm^{-1} are due to O and Al, with a major contribution of O than Al. As we can see from Fig. 3, the PDOS over 729 cm^{-1} are predominantly due to O motions. In the case of $ZnGa_2O_4$, frequencies below 362 cm^{-1} are dominated by the motion of Zn and Ga atoms (with a higher contribution of Ga ions from 261 to 362 cm^{-1}, while higher frequencies are dominated by the motion of O ions, as in $ZnAl_2O_4$). The main difference between the two compounds is due to the fact that Ga atoms are heavier than Al atoms. In the case of $ZnAl_2O_4$ we found a good agreement with the phonon spectrum and PDOS calculated in [24].

The calculated phonon frequencies at ambient pressure in the Γ point are listed in Table 1. Figure 4 a) shows the experimental Raman spectra at room temperature (RT) of $ZnAl_2O_4$ samples up to 13 GPa. Clearly, two Raman modes out of the five Raman-active modes of the spinel phase have been measured and followed under pressure. They are the E_g mode at 418 cm^{-1}, and the T_{2g} mode at 659 cm^{-1} at ambient pressure. These Raman modes agree in frequency with those observed by Chopelas et al. [23]. We have

Table 1 Calculated vibrational modes (cm^{-1}) for $ZnAl_2O_4$ and $ZnGa_2O_4$ at zero pressure in the Γ point [6].

$ZnAl_2O_4$				$ZnGa_2O_4$			
T_{2u}	250	T_{1u}(IR)	548	T_{2u}	135	T_{1u}(IR)	429
T_{1u}(IR)	222	T_{2u}	484	T_{1u}(IR)	175	T_{2u}	450
T_{2g}(R)	194	T_{2g}(R)	513	T_{2g}(R)	186	T_{2g}(R)	488
E_u	402	E_u	600	E_u	229	E_u	563
T_{1u}(IR)	496	T_{1u}(IR)	666	T_{1u}(IR)	342	T_{1u}(IR)	580
T_{1g}	371	T_{2g}(R)	655	T_{1g}	366	T_{2g}(R)	618
E_g(R)	427	A_{2u}	769	E_g(R)	395	A_{2u}	702
A_{2u}	672	A_{1g}(R)	775	A_{2u}	419	A_{1g}(R)	717

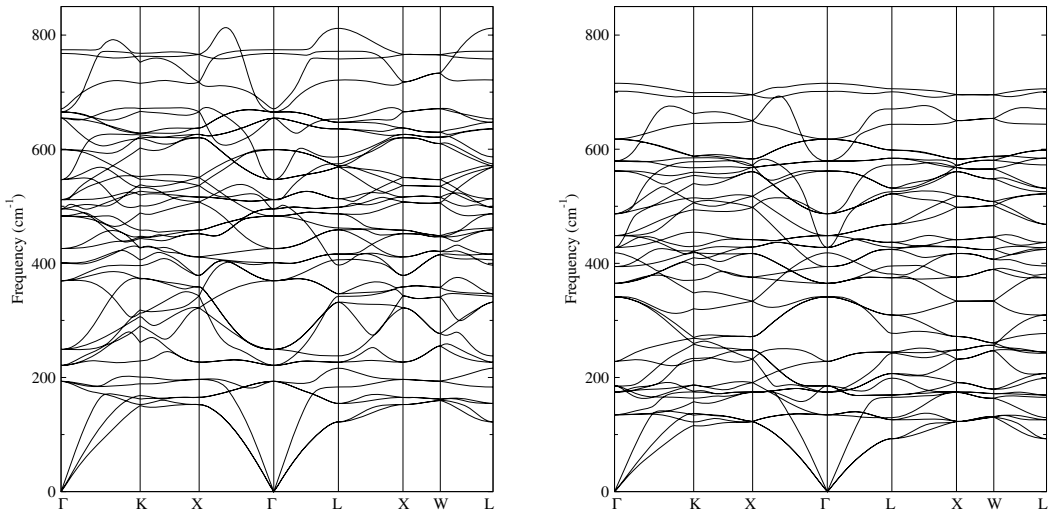

Fig. 2 Calculated phonon-dispersion curves along high-symmetry directions in BZ for a) $ZnAl_2O_4$ and b) $ZnGa_2O_4$.

observed other modes at 155, 488, 708 cm^{-1}, but from these modes Chopelas et al. only found the mode near 708 cm^{-1}.

Table 2 summarizes the calculated and experimental Raman modes with their corresponding pressure coefficients and Grüneisen parameters. A good agreement is found between calculated and experimentally measured Raman mode frequencies and pressure coefficients. The T_{2g} mode calculated to be near 194 cm^{-1} perhaps corresponds to a small peak at 195 cm^{-1} observed as a shoulder of the broad Raman feature extending from 140 to 200 cm^{-1}, whose peak maximum is around 155 cm^{-1}. The pressure dependence of the small peak at 195 cm^{-1} has not been measured but the pressure coefficient of the 155-cm^{-1} peak is around 0.9 cm^{-1}/GPa, which is close to the calculated pressure coefficient for the T_{2g} mode. We have found no clear evidence of the T_{2g} mode calculated to be near 513 cm^{-1} and experimentally found at 509 cm^{-1} by Chopelas et al. Similarly, we have not observed the A_{1g} mode calculated to be near 775 cm^{-1} and experimentally measured around 758 cm^{-1} by Chopelas et al. Instead, we have found two well defined peaks near 488 and 708 cm^{-1} that broaden considerably with increasing pressure. These two features shift at rates of around 7 and 3.8 cm^{-1}/GPa, respectively.

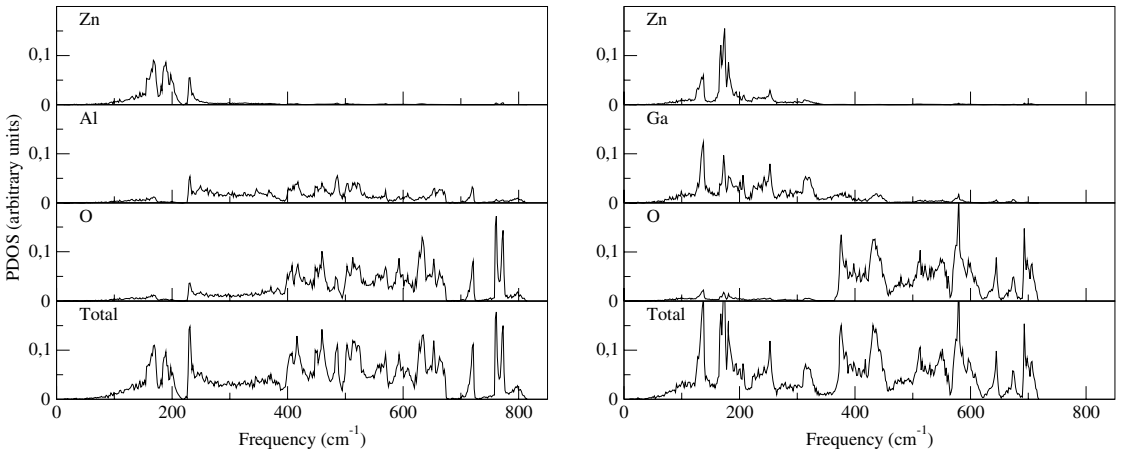

Fig. 3 Partial and total PDOS for a) $ZnAl_2O_4$ and b) $ZnGa_2O_4$ cubic spinels.

Table 2 *Ab initio* calculated and experimental zero pressure frequencies ω (cm^{-1}), Grüneisen parameters γ, and pressure coefficients (cm^{-1}/GPa) of the Raman modes in the cubic spinel structure of $ZnAl_2O_4$ and $ZnGa_2O_4$. Where superscripts refer to ^{a}this work, ^{b} [24], ^{c} [23], ^{d} [25].

	$ZnAl_2O_4$							$ZnGa_2O_4$					
	Theory				Exp.			Theory			Exp.		
Mode	ω^a	γ^a	$\frac{d\omega^a}{dP}$	ω^b	ω^a	$\frac{d\omega^a}{dP}$	ω^c	ω^a	γ^a	$\frac{d\omega^a}{dP}$	ω^a	$\frac{d\omega^a}{dP}$	ω^d
T_{2g}	194	0.9	0.6	197			196	186	1.0	0.7			
E_g	427	1.2	2.0	442	418	2.2	417	395	1.2	1.8			638
T_{2g}	513	1.5	3.0	520			509	488	1.8	3.4	465	3.5	467
T_{2g}	655	1.4	3.4	665	659	3.8	658	618	1.5	3.4	608	3.7	611
A_{1g}	775	1.3	3.8	785			758	717	1.5	4.0	710	4.4	714

Table 2 also summarizes the experimental and theoretical results for the Raman modes of $ZnGa_2O_4$. In this compound, we have also found three out of the five Raman-active modes. There is a good agreement between the experimental and calculated frequencies and pressure coefficients. Our measured and calculated frequencies at zero pressure are also in good agreement with those measured by Van Gorkom et al. [25]. For completeness, Table 3 summarizes the frequencies and pressure coefficients of the IR-active modes in both cubic spinels. Our calculated IR-active mode frequencies compare reasonably well with those experimentally measured by Van Gorkom et al. and Chopelas et al. We have not found any reference in the literature about the pressure dependence of the IR-active modes in both cubic spinels. It is interesting to note that the low-frequency mode associated to vibrations of the octahedral BO_6 units has a considerable smaller pressure coefficient than the other modes not only in $ZnAl_2O_4$ and $ZnGa_2O_4$ but also in $ZnFe_2O_4$ and $ZnCr_2O_4$ [26, 27]. Another systematic behavior we would like to stress is that the high-frequency stretching mode of the ZnO_4 tetrahedral groups has larger pressure coefficients than the bending modes associated to these groups. The first feature is related to the fact that Zn-O bonds are shorter than the *B*-O bonds in all spinel oxides, the second one suggest that in spinels bond stretching has larger force constants than bond bending.

Table 3 *Ab initio* calculated and experimental zero pressure frequencies ω (cm^{-1}), Grüneisen parameters γ, and pressure coefficients (cm^{-1}/GPa) of the IR modes in the cubic spinel structure of $ZnAl_2O_4$ and $ZnGa_2O_4$. Where superscripts refer to [a] this work, [b] [24], [c] [23], [d] [25]. Frequencies from [23, 24] are listed as TO(LO).

	$ZnAl_2O_4$					$ZnGa_2O_4$			
	Theory				Exp.	Theory			Exp.
Mode	ω^a	γ^a	$\frac{d\omega^a}{dP}$	ω^b	ω^c	ω^a	γ^a	$\frac{d\omega^a}{dP}$	ω^d
T_{1u}	222	0.44	0.34	226(240)	220(231)	175	0.06	0.00	175
	496	1.44	2.72	507(528)	440(533)	342	1.26	1.63	328
	548	1.32	2.74	562(648)	543(608)	429	1.54	2.52	420
	666	1.57	4.01	675(832)	641(838)	580	1.89	4.30	570

A curious feature is that our calculations suggest a non-linear behavior of the Raman and IR active modes under pressure in both spinels (see Fig. 5). The non-linear behavior under pressure is very clear in the second IR T_{1u} mode of $ZnAl_2O_4$ and the first IR T_{1u} mode of $ZnGa_2O_4$. From Fig. 5 it is observed that there is a subtle change in slope of the frequencies around 20 GPa in $ZnAl_2O_4$ and around 10 GPa in $ZnGa_2O_4$.

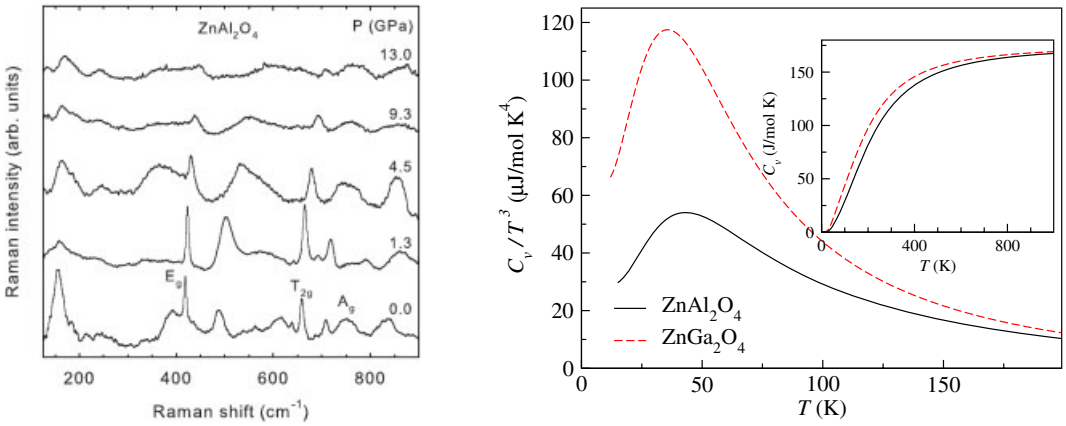

Fig. 4 (online colour at: www.ann-phys.org) a) RT Raman scattering spectra of $ZnAl_2O_4$ up to 13 GPa; b) Temperature dependence of C_v/T^3 per f.u. of $ZnAl_2O_4$ and $ZnGa_2O_4$ of $Fd\bar{3}m$ phase, the inset corresponds to the specific heat vs temperature up to 900 K.

Thermodynamics properties of the crystal at constant volume are determined by the phonons. Calculations of the C_v were performed by integrating the phonon DOS with the standard method [18] (in the region of our interest $C_p \approxeq C_v$). Figure 4 b) shows the temperature dependence of C_v/T^3 per f.u. of $ZnAl_2O_4$ and $ZnGa_2O_4$ in the $Fd\bar{3}m$ phase while the inset shows the C_v evolution with temperature. According to Fig. 4 b) the specific heat C_v at room temperature is 117.16 J/mol·K for $ZnAl_2O_4$, in good agreement with the theoretical value of 116.2 J/mol·K obtained in [24], while the C_v for $ZnGa_2O_4$ is 128.65 J/mol·K. Our results show that the maximum of C_v/T^3 plot is of 53.8 μJ/mol·K^4 for $ZnAl_2O_4$ and 117.4 μJ/mol·K^4 for $ZnGa_2O_4$. Both compounds have the maximum around the value of 43 and 36 K, respectively, showing the clear dependence of the maximum value with the cation. To our knowledge no experimental data are

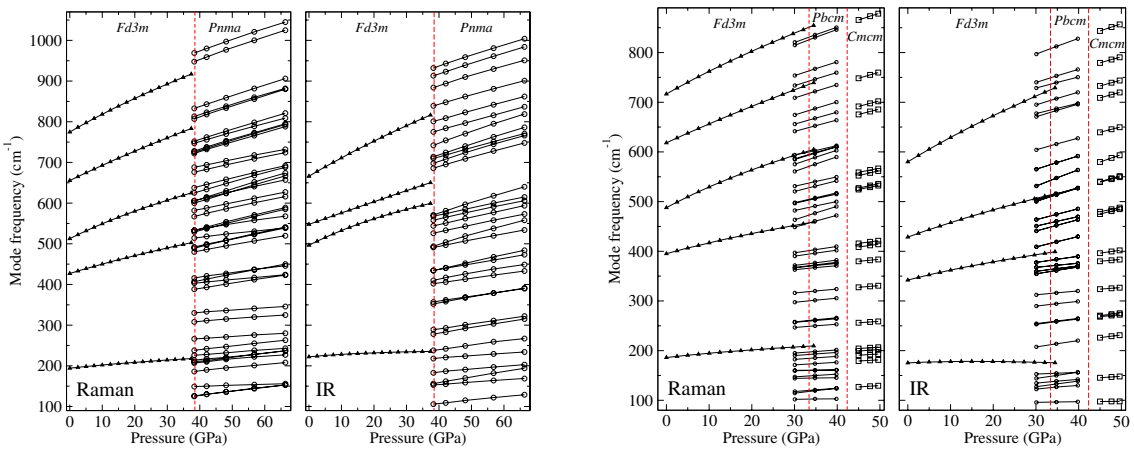

Fig. 5 (online colour at: www.ann-phys.org) Pressure dependence of Raman and IR active modes of space groups a) $Fd\bar{3}m$ and *Pnma* of $ZnAl_2O_4$, and b) $Fd\bar{3}m$, *Pbcm*, and *Cmcm* of $ZnGa_2O_4$.

available, but recent works from Cardona et al. [28,29] found a good agreement between experimental data and similar *ab initio* results in binary compounds.

4.2 High-pressure phases

According to our previous calculations [6,7], a phase transition in $ZnAl_2O_4$ from the cubic spinel towards the $CaFe_2O_4$-type structure (*Pnma*) should occur at 38.5 GPa. Similarly, a phase transition in $ZnGa_2O_4$ from the cubic spinel towards the $CaMn_2O_4$-type structure (*Pbcm*) should occur at 33.4 GPa. In the previous results we found that *Pbcm* structure is very competitive energetically with the $CaTi_2O_4$-type structure (*Cmcm*) due to the close group-subgroup relation between *Cmcm* and *Pbcm* space groups. In this work we found that phonon frequencies from *Pbcm* phase of $ZnGa_2O_4$ have a remarkable change at 42.5 GPa. Due to the close competition of $CaMn_2O_4$- and $CaTi_2O_4$-type structure we think that the $CaTi_2O_4$-type structure becomes more stable than $CaMn_2O_4$-type structure at this pressure. These results suggest a possible second order phase transition with no change in volume at the phase transition pressure. In this transition there is not a change in coordination in Zn and Ga cations (i.e. the $ZnGa_2O_4$ are made up of GaO_6 distorted octahedra and ZnO_8 zinc-centered distorted polyhedra, see Fig. 1). The transition from the *Pbcm* to *Cmcm* phase in ABO_4 compounds has been observed previously in $CaMn_2O_4$ at 35 GPa [30]. In the light of these results we also include the vibrational properties of the $CaTi_2O_4$-type structure of the $ZnGa_2O_4$ compound.

The high pressure phase of $ZnGa_2O_4$, the $CaMn_2O_4$-type structure (SG:*Pbcm*), is characterized by the Wyckoff positions (WPs) $4d$ (x, y, $1/4$) for Zn atom, $8e$ (x, y, z) for Ga atom, and $4c$ (x, $1/4$, 0), $4d$ and $8e$ for O atoms. On the other hand, the $CaTi_2O_4$-type structure (SG: *Cmcm*) is characterized by the following WPs: Zn atoms in $4c$ (0, y, $1/4$), Ga atoms in $8f$ (0, y, z), and O atoms in $4b$ (0, $1/2$, 0), $4c$ and $8f$. Group theory predicts the following vibrations at the Γ point in the *Pbcm* and *Cmcm* phases, respectively

$$\Gamma(Pbcm) = 11A_g(R) + 9A_u + 12B_{1g}(R) + 10B_{1u}(IR) + 10B_{2g}(R) + 12B_{2u}(IR) + 9B_{3g}(R) + 11B_{3u}(IR)$$

$$\Gamma(Cmcm) = 6A_g(R) + 3A_u + 4B_{1g}(R) + 8B_{1u}(IR) + 2B_{2g}(R) + 8B_{2u}(IR) + 6B_{3g}(R) + 5B_{3u}(IR)$$

In the $CaFe_2O_4$-type structure of $ZnAl_2O_4$ the Zn, Al and O atoms occupy the WP 4*c* (x, $1/4$, z), in which Al and O atoms have two and four different 4*c* WPs, respectively. Group theory predicts the following vibrations at the Γ point in the *Pnma* phase

$$\Gamma(Pnma) = 14A_g(R) + 7A_u + 7B_{1g}(R) \\ +14B_{1u}(IR) + 14B_{2g}(R) + 7B_{2u}(IR) + 7B_{3g}(R) + 14B_{3u}(IR)$$

In Table 4 appears the mechanical representation of the phonon modes of the space groups $Pbcm$, $Pnma$, and $Cmcm$ in which is clearly depicted the corresponding modes to each Wyckoff position.

Table 4 Mechanical representation of the phonon modes of the space groups (SG) $Pbcm$, $Pnma$, and $Cmcm$, which correspond to the $CaMn_2O_4$-, $CaFe_2O_4$-, and $CaTi_2O_4$-type structures. Where A_g and B_{xg} are Raman modes and B_{xu} are IR modes.

SG	WP	A_g	A_u	B_{1g}	B_{1u}	B_{2g}	B_{2u}	B_{3g}	B_{3u}
$Pbcm$	8e	3	3	3	3	3	3	3	3
	4d	2	1	2	1	1	2	1	2
	4c	1	1	2	2	2	2	1	1
$Pnma$	4c	2	1	1	2	2	1	1	2
$Cmcm$	8f	2	1	1	2	1	2	2	1
	4c	1		1	1		1	1	1
	4b		1		2		2		1

Table 5 summarizes the different modes, frequencies, pressure coefficients and Gruneisen parameters for $ZnAl_2O_4$ in the *Pnma* structure at 42.1 GPa and $ZnGa_2O_4$ in the *Pbcm* structure at 34.8 GPa. Correspondingly, Table 6 summarizes the different modes, frequencies, pressure coefficients and Gruneisen parameters for $ZnGa_2O_4$ in the *Cmcm* structure at 45 GPa. The calculated pressure dependence of the Raman- and IR-active modes of the *Fd*$\bar{3}$*m* and Pnma phases in $ZnAl_2O_4$ and of the *Fd*$\bar{3}$*m*, *Pbcm*, and *Cmcm* in $ZnGa_2O_4$ are plotted in Figs. 5a) and b), respectively.

According to group theory, there are four types of Raman active modes (A_g, B_{1g}, B_{2g}, B_{3g}) and three types of IR active modes (B_{1u}, B_{2u} and B_{3u}) in the *Pbcm*, *Pnma*, *Cmcm* space groups. With the correlation between the Raman active modes of the four point groups (*Fd*$\bar{3}$*m* and *Pbcm*, *Pnma*, *Cmcm*) the A_{1g} and E_g modes in the *Fd*$\bar{3}$*m* representation transform to the A_g modes in the *Pbcm*, *Pnma* and *Cmcm* representation, and the T_{2g} modes transform to the B_{1g} + B_{2g} + B_{3g} modes. The correlation of some of the vibrational modes in the different phases can be followed in our calculations.

For the spinel structure of $ZnGa_2O_4$, the first T_{2g} Raman mode has a pressure coefficient of 0.66 cm^{-1}/GPa, for *Pbcm* phase the Raman modes below 403 cm^{-1} (A_g from Table 5) have pressure coefficients between 0.09 and 1.29 cm^{-1}/GPa, and the *Cmcm* phase have pressure coefficients between 0.52 and 1.22 cm^{-1}/GPa for frequencies lower than 416 cm^{-1} (A_g). For this range of frequency we find that in the *Pbcm* and *Cmcm* phases there are many Raman modes with pressure coefficient values very close to the first mode T_{2g} of cubic spinel. After a frequency of 460 cm^{-1} pressure coefficients increase from 1.82 to 3.2 and 1.72 to 2.76 cm^{-1}/GPa for *Pbcm* and *Cmcm* phases, respectively. Also, it is observed that there are many Raman modes from orthorhombic phases of $ZnGa_2O_4$ that have pressure coefficients with values very close to the respective modes of spinel phase. Similar behavior is observed for $ZnAl_2O_4$ and IR active modes in both compounds.

Table 5 *Ab initio* calculated frequencies ω (cm^{-1}), Grüneisen parameters γ, and pressure coefficients (cm^{-1}/GPa) of the phonon modes of $ZnAl_2O_4$ in the *Pnma* structure, and $ZnGa_2O_4$ in the marokite structure. Frequencies were calculated at 42.1 and 34.8 GPa for $ZnAl_2O_4$ and $ZnGa_2O_4$, respectively. Where A_g and B_{xg} are Raman modes and B_{xu} are IR modes.

$ZnAl_2O_4$								$ZnGa_2O_4$							
	ω	γ	$\frac{d\omega}{dP}$		ω	γ	$\frac{d\omega}{dP}$		ω	γ	$\frac{d\omega}{dP}$		ω	γ	$\frac{d\omega}{dP}$
B_{2u}	-	-	-	A_u	504	1.9	2.2	B_{1u}	-	-	-	B_{1g}	396	1.2	1.2
B_{3u}	-	-	-	A_g	518	0.7	0.9	B_{2u}	-	-	-	A_g	403	1.3	1.3
B_{1u}	-	-	-	B_{3u}	533	1.3	1.7	B_{3u}	-	-	-	A_u	417	2.0	2.1
B_{3u}	109	3.1	0.8	B_{1g}	537	1.6	2.0	A_u	22			B_{1u}	419	2.0	2.1
A_u	110	3.2	0.9	B_{3g}	541	1.6	2.0	B_{1u}	97	0.5	0.1	B_{3u}	452	2.0	2.3
B_{1g}	129	3.1	1.0	A_g	539	1.0	1.2	B_{2g}	103	0.4	0.1	B_{3g}	460	2.1	2.4
B_{3g}	130	3.1	1.0	B_{3u}	551	1.4	1.8	A_g	119	3.2	1.0	B_{1u}	460	1.6	1.9
A_u	141	1.6	0.5	B_{1u}	565	1.3	1.7	B_{1g}	121	2.1	0.7	A_u	468	1.6	1.9
A_g	150	0.7	0.2	A_u	577	1.8	2.5	B_{2u}	127	2.3	0.7	A_g	477	2.3	2.7
B_{1u}	155	1.6	0.6	B_{2g}	575	1.3	1.7	B_{1u}	133	3.4	1.1	B_{2u}	474	1.9	2.2
B_{2u}	162	3.4	1.3	B_{1u}	574	1.2	1.7	A_u	130	1.1	0.4	B_{2g}	491	1.5	1.8
B_{3u}	186	1.6	0.7	B_{2u}	581	1.8	2.5	B_{3u}	138	2.2	0.8	A_g	506	1.5	1.9
A_g	190	1.7	0.8	A_g	588	1.6	1.6	B_{1g}	145	0.3	0.1	B_{2g}	507	1.5	2.0
A_u	205	1.6	0.8	B_{1g}	609	1.6	2.4	B_{2u}	150	3.3	1.3	B_{1u}	514	2.1	2.7
B_{2g}	210	1.5	0.7	B_{3g}	615	1.7	2.5	B_{2g}	150	1.5	0.6	B_{2u}	516	1.8	2.4
A_g	213	1.9	1.0	B_{2g}	613	1.3	1.8	B_{3u}	154	0.8	0.3	B_{1g}	531	1.6	2.2
B_{2g}	217	1.6	0.8	A_g	634	1.5	2.3	A_u	161	1.0	0.4	A_u	543	2.5	3.4
B_{2u}	221	1.1	0.6	B_{2g}	646	1.3	1.9	B_{3g}	160	0.3	0.1	B_{3g}	540	1.4	1.9
B_{1g}	228	1.2	0.6	A_g	683	1.1	1.7	A_g	161	0.2	0.1	B_{3u}	547	2.4	3.3
B_{1u}	242	1.8	1.0	B_{3u}	695	1.3	2.2	A_g	174	1.2	0.5	B_{3g}	575	2.0	3.0
B_{2g}	242	1.5	0.9	B_{2g}	694	1.0	1.6	B_{3g}	185	1.3	0.6	B_{3u}	578	1.8	2.7
B_{3g}	268	0.8	0.5	B_{1u}	708	1.5	2.4	B_{2g}	193	1.3	0.6	A_g	589	1.9	2.8
B_{1u}	283	1.9	1.3	A_u	716	1.3	2.2	B_{1g}	198	1.3	0.6	B_{2g}	597	1.7	2.6
B_{3u}	293	1.7	1.2	B_{2u}	718	1.3	2.2	B_{1u}	214	2.4	1.3	B_{1g}	599	1.6	2.5
B_{3g}	311	0.8	0.6	B_{1u}	724	1.5	2.6	B_{3g}	250	1.0	0.6	B_{1g}	602	1.2	1.9
B_{1g}	333	0.7	0.6	B_{3g}	732	1.3	2.3	B_{2u}	258	1.7	1.1	B_{2u}	616	1.5	2.4
B_{3u}	358	1.6	1.4	A_g	735	1.4	2.4	B_{2u}	259	1.6	1.1	A_u	618	1.4	2.2
B_{1u}	362	1.4	1.2	B_{1g}	738	1.4	2.4	B_{2g}	260	1.1	0.7	B_{3g}	652	1.4	2.3
A_g	393	1.3	1.2	B_{3u}	754	1.5	2.7	B_{1g}	262	1.3	0.8	A_g	668	1.4	2.4
B_{3u}	406	1.2	1.1	B_{2g}	756	1.2	2.2	B_{3u}	294	1.3	1.0	B_{1u}	683	1.5	2.6
B_{2g}	406	0.8	0.7	A_g	762	1.4	2.4	B_{1g}	301	1.1	0.8	B_{2g}	687	1.5	2.6
A_g	413	1.6	1.5	B_{3u}	784	1.2	2.2	B_{1u}	316	1.0	0.8	B_{3u}	687	1.2	2.1
B_{1u}	417	1.4	1.4	B_{1u}	809	1.1	2.2	A_g	320	1.0	0.8	B_{2u}	707	1.4	2.6
B_{2g}	421	1.1	1.1	A_g	818	1.3	2.6	A_u	331	1.0	1.6	A_g	722	1.5	2.7
B_{2u}	441	1.7	1.8	B_{2g}	823	1.3	2.5	B_{3u}	361	1.5	1.4	B_{3u}	739	1.2	2.2
B_{1u}	440	1.3	1.4	B_{2g}	843	1.3	2.6	B_{2u}	365	1.2	1.1	B_{1g}	746	1.4	2.7
A_u	456	1.7	1.8	B_{1u}	848	1.1	2.2	B_{2g}	367	0.9	0.8	B_{2u}	753	1.4	2.7
B_{2g}	486	1.2	1.4	B_{3u}	894	1.1	2.4	B_{3g}	371	0.9	0.9	B_{1g}	767	1.4	2.8
B_{3g}	497	1.5	1.8	B_{3u}	923	1.2	2.5	B_{1g}	372	1.1	1.1	B_{1u}	812	1.5	3.2
B_{3u}	497	1.3	1.5	B_{1u}	943	1.2	2.6	B_{2u}	372	0.9	0.8	A_u	813	1.4	3.0
B_{1g}	498	1.5	1.7	A_g	959	1.2	2.7	A_g	377	1.1	1.1	B_{2g}	830	1.5	3.2
B_{2u}	504	1.9	2.3	B_{2g}	980	1.2	2.7	B_{3u}	384	1.3	1.3	B_{3g}	835	1.4	3.1

Table 6 *Ab initio* calculated frequencies ω (cm^{-1}), Grüneisen parameters γ, and pressure coefficients (cm^{-1}/GPa) of the phonon modes of $ZnGa_2O_4$ in the *Cmcm* structure at 45 GPa.

Mode	ω	γ	$\frac{d\omega}{dP}$	Mode	ω	γ	$\frac{d\omega}{dP}$
B_{2u}	-	-	-	A_g	416	1.2	1.2
B_{1u}	-	-	-	A_u	438	1.9	1.9
B_{3u}	-	-	-	B_{3u}	475	2.0	2.1
A_u	31			B_{1u}	479	1.7	1.8
B_{1u}	98	0.3	0.1	A_g	524	1.4	1.7
B_{1g}	127	1.8	0.5	B_{2g}	527	1.5	1.8
B_{3u}	145	1.7	0.6	B_{2u}	539	1.8	2.2
A_g	179	1.2	0.5	B_{1u}	540	2.0	2.4
B_{3g}	191	1.1	0.5	B_{1g}	552	1.6	2.0
B_{2g}	199	1.2	0.6	B_{3g}	559	1.4	1.7
B_{1g}	204	1.2	0.5	A_u	576	2.3	3.0
B_{1u}	226	2.1	1.1	B_{3u}	580	2.2	3.0
B_{3g}	256	1.0	0.6	B_{2u}	640	1.5	2.2
B_{2u}	268	1.4	0.8	B_{3g}	675	1.4	2.1
B_{2u}	271	1.7	1.0	A_g	692	1.4	2.2
B_{1u}	324	0.9	0.6	B_{1u}	709	1.5	2.4
A_g	327	0.9	0.7	B_{2u}	733	1.4	2.4
B_{3g}	380	0.9	0.8	A_g	748	1.5	2.5
B_{2u}	380	0.9	0.7	B_{2u}	779	1.4	2.5
B_{3u}	396	1.3	1.2	B_{1u}	843	1.5	2.8
B_{1g}	409	1.3	1.2	B_{3g}	866	1.4	2.8

5 Conclusions

We have calculated by first principles the Raman and IR phonon modes as well as the pressure coefficients and Grüneisen parameters of the spinel structure in the range of pressure from 0 to 35 GPa for $ZnAl_2O_4$ and $ZnGa_2O_4$. Additionally we have measured the Raman spectra of these two spinels up to 12 GPa and we have found a good agreement between our experimental and theoretical data and with available data in the literature. Finally, we have calculated the pressure dependence of the Raman and IR active modes in other high-pressure structures (the orthorhombic $CaMn_2O_4$-, $CaFe_2O_4$-, and $CaTi_2O_4$-type structures) of these two spinels and we have found the possibility of a second order phase transition in $ZnGa_2O_4$ from the $CaMn_2O_4$- to a $CaTi_2O_4$-type structure around of 42.5 GPa which was not found in our previous report [6].

We hope that this work will stimulate and help future theoretical and experimental studies of phonon frequencies of AB_2O_4 compounds.

Acknowledgements In this work we have studied the effect of pressure to the lattice dynamics of $ZnAl_2O_4$ and $ZnGa_2O_4$ spinels under pressure. It is a tribute to Manuel Cardona, who has contributed (between many others) to the fields of systems under pressure and optical spectroscopies. In particular, in the high pressure science, he has contributions of the order of 300 papers, which indicates his strong involvement with the field.

A.H.R. has been supported by CONACyT México under the project J-59853-F, PROALMEX-DAAD-CONACYT, Spain and CGSTIC – Cinvestav. S. L.-M. acknowledge the support of the CONACyT México by the postdoctoral fellowship. F.J.M., D.E., P. R.-H. and A. M. acknowledge the financial support of the MICINN of Spain under grants Nos. MAT2007-65990-C03-03/01, MAT2010-21270-C04-01/03/04, CSD2007-00045, and the computer resources provided by RES (Red Española de Supercomputación) Spain and Kan Balam Supercomputer, UNAM, México.

References

[1] T. Omata, N. Ueda, K. Ueda, and H. Kawazoe, Appl. Phys. Lett. **64**, 1077 (1994).
[2] S. Sampath and J. Cordaro, J. Am. Ceram. Soc. **81**, 649 (1998).
[3] B. Cheng, S. Qu, H. Zhou, and Z. Wang, Nanotech. **17**, 2982 (2006).
[4] D. Levy, A. Pavese, A. Sani, and V. Pischedda, Phys. Chem. Miner. **28**, 612 (2001).
[5] D. Errandonea et al., Phys. Rev. B **79**(2), 024103 (2009).
[6] S. López et al., Phys. Rev. B **79**, 214103 (2009).
[7] S. López-Moreno, A. H. Romero, P. Rodríguez-Hernández, and A. Muñoz, High Press. Res. **29**(4), 573–577 (2009).
[8] S. Åsbrink et al., Phys. Rev. B **60**(18), 12651–12656 (1999).
[9] S. Åsbrink, A. Waśkowska, J. S. Olsen, and L. Gerward, Phys. Rev. B **57**(9), 4972–4974 (1998).
[10] P. Blochl, Phys. Rev. B **50**, 17953 (1994).
[11] G. Kresse and D. Joubert, Phys. Rev. B **59**, 1758 (1999).
[12] G. Kresse and J. Hafner, Phys. Rev. B **47**, 558 (1993).
[13] G. Kresse and J. Hafner, Phys. Rev. B **49**, 14251 (1994).
[14] G. Kresse and J. Furthmüller,Comput. Math. Sci. **6**, 15 (1996).
[15] G. Kresse and J. Furthmüller,Phys. Rev. B **54**, 11169 (1996).
[16] J. Perdew and A. Zunger, Phys. Rev. B **23**, 5048 (1981).
[17] H. Monkhorst and J. Pack, Phys. Rev. B **13**, 5188 (1976).
[18] K. Parlinski, Computer Code PHONON. See: http://wolf.ifj.edu.pl/phonon.
[19] A. Phani et al., J. Mater. Sci. **33**, 3969 (1998).
[20] E. Rusu et al., Phys. Status Solidi C **6**, 1199 (2009).
[21] D. Errandonea, Y. Meng, M. Somayazulu, and D. Hüsermann, Physica B **355**, 116 (2005).
[22] H. Mao, J. Xu, and P. Bell, J. Geophys. Res. **91**, 4673 (1986).
[23] A. Chopelas and A. Hofmeister, Phys. Chem. Miner. **18**, 279 (1991).
[24] C. M. Fang, C. K. Loong, G. A. de Wijs, and G. de With, Phys. Rev. B **66**(14), 144301 (2002).
[25] G. V. Gorkom, J. Haanstra, and H. Boom, J. Raman Spectrosc. **1**, 513 (1973).
[26] Z. Wang, D. Schiferl, Y. Zhao, and H. C. O'Neill, J. Phys. Chem. Solids **64**, 2517 (2003).
[27] Z. Wang, P. Lazor, S. K. Saxena, and G. Artioli, J. Solid State Chem. **165**, 165 (2002).
[28] A. Yang, Phys. Rev. B **80**(19), 195203 (2009).
[29] M. Cardona et al., Phys. Rev. B **81**(7), 075207 (2010).
[30] Z. Wang, S. K. Saxena, and J. J. Neumeier, J. Solid State Chem. **170**, 382 (2003).